

Formation rate of $p\mu d$ muon molecules as a function of hydrogen temperature

V. P. Dzhelepov, V. G. Zinov, S. A. Ivanovskii, S. B. Karpov, A. D. Konin, A. I. Malyshev, L. Martsish, D. G. Merkulov, A. I. Rudenko, and V. V. Fil'chenkov

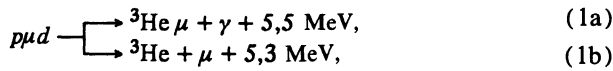
Joint Institute for Nuclear Research

(Submitted 12 June 1992)

Zh. Eksp. Teor. Fiz. **103**, 730–739 (March 1993)

Using a high-pressure (0.6 kbar) cryogenic target in the muon beam of the JINR phasotron, we have measured the temporal distribution of gamma rays from the reaction $p\mu d \rightarrow {}^3\text{He}\mu + \gamma + 5.5 \text{ MeV}$ in an 98.3% $\text{H}_2 + 1.7\% \text{D}_2$ mixture over the temperature range $T = 21\text{--}300 \text{ K}$. Analysis of the results yields the formation rate $\lambda_{p\mu d}$ of $p\mu d$ molecules and the rate of the $p + d$ reaction in the $p\mu d$ system. The data thus obtained suggest that $\lambda_{p\mu d}$ is temperature independent. The temperature-averaged value, $\lambda_{p\mu d} = 5.49 \pm 0.30 \mu\text{s}^{-1}$, is in good agreement with theory and with other measurements conducted at $T = 20$ and 300 K .

The muon-catalyzed deuterium cycle is of interest primarily because of the spin dependence of the reaction



which can proceed in the $p\mu d$ molecule from either of two total-spin states of the proton plus deuteron, $S_{pd} = 3/2$ or $S_{pd} = 1/2$. By varying the experimental setup (changing the concentration of the components, for example), we can alter the populations of these states, thereby changing the outcome of the reaction (Gershtein–Wolfenstein effect^{1–3}). Recent studies of that effect and an interpretation based on new calculations^{4,5} of the $p + d$ reaction rates may be found in Refs. 5 and 6. There is still a problem with this interpretation, however, in explaining measurements of the absolute gamma-ray yield obtained in a number of previous experiments.

Another important aspect of the problem relates to the possible temperature dependence of the $p\mu d$ molecule formation rate ($\lambda_{p\mu d}$) in an $\text{H}_2 + \text{D}_2$ mixture, due to a number of “exotic” factors that we now describe. Hara *et al.*⁷ and Matveenko⁷ have pointed out the possibility of resonant behavior (as a function of the energy of the $d\mu$ atom) in the formation cross section of the $p\mu d$ system, due to the presence of a weakly bound level with anomalous parity $P = 1^J$ (where J is the total orbital angular momentum of the $p\mu d$ system); the binding energy is a few electron volts. A state with binding energy 3.5 eV has by now been convincingly predicted by various calculations,^{8,9} but just what the formation rate of the $p\mu d$ molecule in that state would be has yet to be studied.

The possibility of changes in the population of $p\mu d$ molecular states with different values of the total nuclear spin^{10,11} in collisions between a molecular complex containing $(p\mu d)^+$ ions and hydrogen molecules of high enough energy has also been examined. If such changes do take place, then the outcome of reaction (1) ought to depend on the hydrogen temperature and density.

The formation rate of $p\mu d$ molecules was previously measured only in liquid hydrogen at $T = 20 \text{ K}$ ^{3,6,12} and in gaseous hydrogen at room temperature¹³ (see Table I). Those measurements are mutually consistent, but in another experiment¹⁴ (TRIUMF group) that measured the outcome of reaction (1) in gaseous hydrogen, the result varied appreciably with temperature. We therefore thought it worthwhile to measure the formation rate of $p\mu d$ muon molecules over a wide temperature range in $\text{H}_2 + \text{D}_2$.

The processes induced by negative muons in a mixture $(1 - c_d)\text{H}_2 + c_d\text{D}_2$ (c_d is the partial concentration of deuterium) are diagrammed in Fig. 1 (taken from Ref. 6), and the parameters characterizing those processes are listed in Table I.

As usual, the spin-flip rate λ_d in the $d\mu$ atom (for the transition $F_{d\mu} = 3/2 \rightarrow F_{d\mu} = 1/2$) and the formation rate $\lambda_{p\mu d}$ of the $p\mu d$ molecule have been normalized to a liquid hydrogen density $n_0 = 4.25 \times 10^{22} \text{ nucl/cm}^3$. Their instantaneous values, given the actual hydrogen and deuterium densities in the $\text{H}_2 + \text{D}_2$ mixture, are $\Lambda_d = \lambda_d c_d \varphi$ and $\Lambda_{p\mu d} = \lambda_{p\mu d} (1 - c_d) \varphi$, where $\varphi = n/n_0$ is the relative density of the mixture.

The nuclear reaction rate $\lambda_{f,\gamma}^{1/2}$ was derived in Refs. 3, 12, and 17 by analyzing measurements of the gamma-ray yield from reaction (1), assuming (according to current

TABLE I. Parameters of the muon-catalyzed deuterium cycle in $\text{H}_2 + \text{D}_2$ (all quantities in μs^{-1}).

Quantity	λ_d	$\lambda_{p\mu d}$	$\lambda_{f,\gamma}^{3/2}$	$\lambda_{f,\gamma}^{1/2}$
Experiment	30 — 40 [15, 16]	$5,8 \pm 0,3$ [3]	—	$0,305 \pm 0,010$ [3]
		$5,53 \pm 0,16$ [13]	—	$0,287 \pm 0,022$ [17]
		$5,9 \pm 0,9$ [12]	—	$0,289 \pm 0,027$ [12]
		$5,6 \pm 0,2$ [6]	$0,11 \pm 0,01$ [6]	$0,35 \pm 0,02$ [6]
Theory	30 — 40 [18]	$5,6$ [19]	$0,11$ [4]	$0,37 \pm 0,01$ [4]

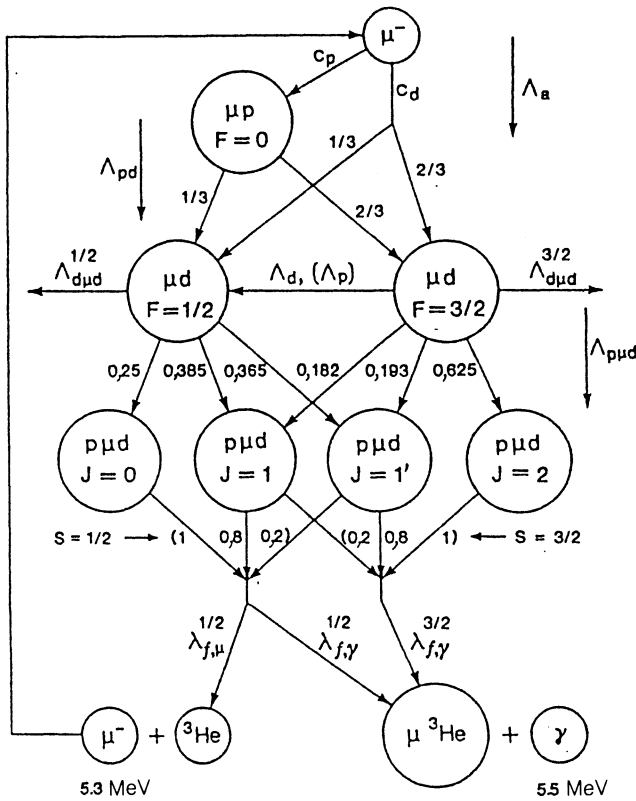


FIG. 1. Processes induced by negative muons in a mixture of hydrogen and deuterium.

opinion) that the reaction rate out of the $S_{pd} = 3/2$ state is negligible. Both rates—for the $S_{pd} = 3/2$ and $S_{pd} = 1/2$ states—were independently obtained in the experiments reported in Ref. 6.

Slowing down in a mixture of hydrogen and deuterium, muons form $p\mu$ and $d\mu$ atoms with initial populations proportional to the partial concentrations $c_p = 1 - c_d$ and c_d . Through the fast exchange process $p\mu + d \rightarrow d\mu + p$, muons are transferred from hydrogen to deuterium in a time $t \approx 10^{-10}/c_d \varphi$, and they populate the hyperfine structure levels of the $d\mu$ atom with statistical weights 2/3 and 1/3. Subsequent interactions of $d\mu$ atoms with deuterons can lead to the transition $F_{d\mu} = 3/2 \rightarrow F_{d\mu} = 1/2$, with corresponding rate Λ_d .

It is clear from Fig. 1 that the relative populations of the four hyperfine states of the $p\mu d$ molecules produced by collisions of $d\mu$ atoms with protons (hydrogen molecules) depend on the spin state of the $d\mu$ atom. Likewise, the $p + d$ nuclear reaction rate is different in each of these states of the

$p\mu d$ molecule. The outcome of this reaction and the overall temporal distribution of its products therefore depend not only on the formation rate $\lambda_{p\mu d}$ of the $p\mu d$ system and the reaction rates in that system ($\lambda_{f,\gamma}^{3/2}$ and $\lambda_{f,\gamma}^{1/2}$), but on the spin-flip rate of the $d\mu$ atom as well.

In the work described here, we have measured and analyzed the characteristics of the 5.5-MeV gamma rays emerging from reaction (1a), using the muon beam of the JINR phasotron. We used a similar experimental setup to study muon catalysis in pure deuterium;^{15,20,21} in the present experiment, one of two neutron detectors was replaced by a NaJ(Tl) gamma-ray scintillation spectrometer 150 mm in diameter and 100 mm long. The detection efficiency for gamma rays from reaction (1a) was $\epsilon_\gamma \approx 3\%$.

We used a high-pressure (0.6 kbar) cryogenic target²² mounted in a cryostat that held the temperature constant to within ± 1.5 K over the range $T = 20$ K to $T = 300$ K. Before beginning a series of measurements, we completely filled the target with a liquid mixture ($T = 21$ K) consisting of 98.3% H_2 and 1.7% D_2 (first run); we then collected data at $T = 21$ –81 K. Some of the gas was then purged from the target and measurements were made at $T = 170$ K. After purging still more of the gas, we made the rest of the measurements. The measurement conditions (temperature and density) are shown in Table II, where the run number corresponds to the order in which a measurement was taken.

In our experiments, we detected gamma rays from the $p + d$ fusion reaction in the $p\mu d$ molecule, neutrons from the reaction $d + d \rightarrow {}^3He + n$ in the $d\mu d$ molecule, and for normalization, electrons from muon decay in deuterium. For subsequent computer processing, we removed events registered by the gamma or neutron detectors. The signal from stopped muons was eliminated by a 10- μs anticoincidence gate, which required that signals be present during that time from the neutron (n) and electron (e) detectors. Suppression of the background associated with stopped muons in the target walls also required that $t_e - t_0 > 0.5 \mu s$, where t_e is the time at which the decay electron is detected and t_0 is the time at which the muon is stopped in the target.

In these experiments, we determined the time-varying hydrogen density in the target by using the normalized electron yield from mu decay in hydrogen as measured in the various runs. The yield obtained in the first run ($T = 21$ K, $\varphi = 1$), for which the density was accurately known, was used as a reference point. The electron yield from mu decay in hydrogen (the area under an exponential with time constant $\tau = 2.2 \mu s$) was normalized to the electron yield from mu decay in the target walls ($\tau = 0.2 \mu s$). We used a timing analyzer to measure the electron spectra. We note here that when the amount of hydrogen in the target remained con-

TABLE II. Measurement conditions for $H_2 + D_2$ runs.

Parameter	Run							
	1	2	3	4	5	6	7	8
Temperature, K	21	48	81	170	94	165	220	302
Density, φ	1.0	0.99	0.99	0.67	0.41	0.41	0.41	0.41
Number of gamma rays, N_γ	4356	2959	3303	3197	1825	2020	1987	1872
Number of electrons, $N_e \cdot 10^{-3}$	309	211	247	235	146	153	159	156

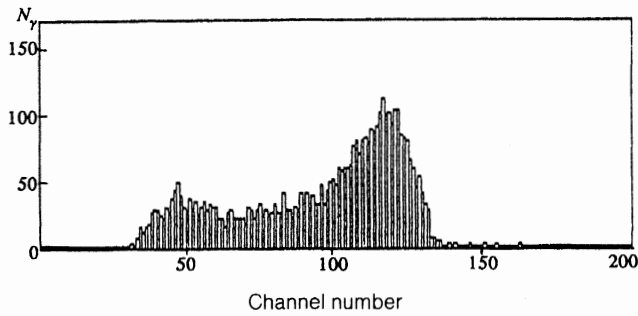


FIG. 2. Amplitude distribution of gamma rays from reaction (1a) measured at $T = 21$ K.

stant, the measured value of the normalized electron yield varied by less than 1% from one run to the next.

In addition to measurements in hydrogen, we also obtained data with helium and vacuum targets in order to determine the gamma-ray and electron backgrounds. The number of detected gamma rays (N_γ) shown in Table II corresponds to $t_e - t_\gamma = 0.5\text{--}2.5 \mu\text{s}$, the decision criterion used in the final processing (t_γ is the detection time for gamma rays); the background has already been subtracted. The background contributes no more than 5% with the adopted selection criteria. In Table II, N_e denotes the number of electrons detected by the gamma detector. In Fig. 2, we have plotted the amplitude, and in Fig. 3, the temporal distribution of gamma rays detected in the run at $T = 21$ K; the data are well fit by theory.

The abundance C_Z of contaminants with $Z > 1$ in the hydrogen was determined by analyzing the temporal distribution of electrons detected in runs 1–8; these spectra were fit by an expression of the form $(dN_e/dt)\exp(-\lambda_e t)$. For the first five runs, λ_e was found to equal the muon decay rate $\lambda_0 = 0.455 \mu\text{s}^{-1}$ to within 0.4%, implying that the probability of a contaminant capturing a muon from a $d\mu$ atom in those runs was less than 2–3%. The data of the last three runs suggest that the corresponding probability was approximately 6–7%. The results were corrected appropriately.

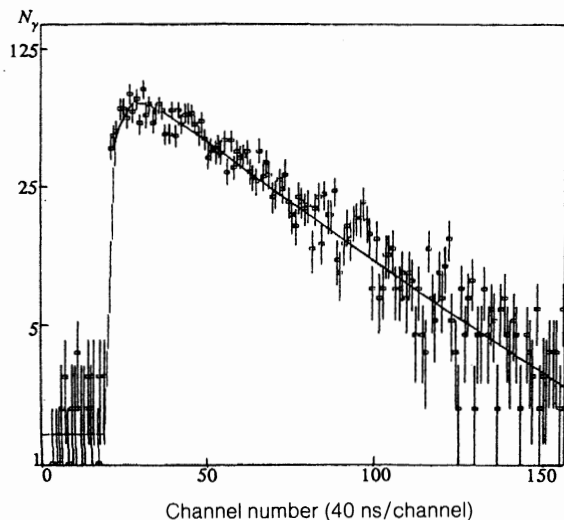


FIG. 3. Amplitude distribution of gamma rays from reaction (1a) measured at $T = 21$ K. The curve is the best fit of the form (3).

The experimentally observed dynamics of hydrogen contamination probably derive from the gradual dissolution in hydrogen of impurities that were present in condensed form at lower temperatures.

The relative yield of gamma rays $\eta_\gamma = N_\gamma/N_e$ derived from the data in Table II has been plotted in Fig. 4, which shows the main yield for $\varphi = 0.4$ (solid line) and $\varphi = 1.0$ (dashed line). The difference between the two is consistent with the difference calculated by taking the overall kinetics of the processes into consideration. To within about 1–2%, the difference factor can be estimated by using the expression

$$W_{p\mu d} = \lambda_{p\mu d}(1 - c_d)\varphi / [\lambda_0 + \lambda_{p\mu d}(1 - c_d)\varphi + \Lambda_Z] \quad (2)$$

for the probability of $p\mu d$ molecule formation as a function of hydrogen density (here Λ_Z is the rate of gamma captures by impurities).

We see from Eq. (2) that in high-density hydrogen, with $\Lambda_{p\mu d} \gg \lambda_0$, the gamma yield is a weak function of $\lambda_{p\mu d}$; it is, however, sensitive to $\Lambda_Z = \lambda_Z C_Z \varphi$. This makes it possible to determine the magnitude of the impurity-related gamma-capture corrections by combining an analysis of the temporal distribution of gamma rays and electrons with an analysis of the relative gamma-ray yield.

The processes depicted in Fig. 1 correspond to a complicated set of differential equations that can only be solved numerically.²³ In our analysis of the temporal distribution of gamma rays, we took advantage of the analytic solution $y_\gamma(t)$ obtained by neglecting muon regeneration in reaction (1). In so doing, we initially assumed that the reaction has a relatively low yield (25%), and that the probability of a muon sticking to ${}^3\text{He}$ is large ($\omega_{pd} \approx 0.85$; Ref. 6), so that altogether regeneration affects the outcome at the 3–4% level.

It can be seen from Fig. 1 that $d\mu$ atoms can also form $d\mu d$ molecules, with a subsequent $d + d$ fusion reaction. Our experimental conditions ($c_d \ll 1$) were such that this channel is suppressed by approximately two orders of magnitude below the reactions in (1). Given the virtually complete regeneration of muons following $d + d$ fusion, it has no effect on our results. Due to the smallness of the effect, we were unable to obtain any reliable data on the temporal distribution of neutrons from the reaction $d + d \rightarrow {}^3\text{He} + n$.

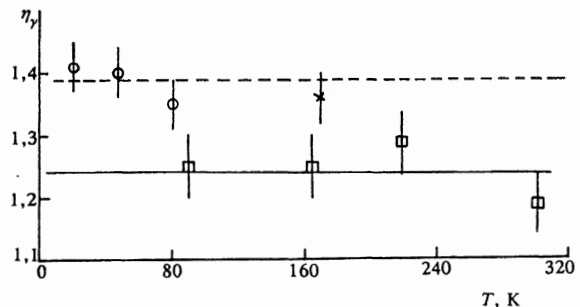


FIG. 4. Relative yield of gamma rays as a function of temperature of the $\text{H}_2 + \text{D}_2$ mixture. Experimental data: \circ —density $\varphi = 1$; \times —measurements at $\varphi = 0.67$; \square —results for $\varphi = 0.41$. The dashed line is the mean value of η_γ for experimental runs with $\varphi = 1$; the solid line is the mean for $\varphi = 0.41$.

The expression that we used for the temporal distribution of gamma rays is

$$y_\gamma(t) = \Lambda_{p\mu d} [y_{\gamma, F=3/2}(t) + y_{\gamma, F=1/2}(t)],$$

$$y_{\gamma, F} = \sum C_{F, J} Z_J(t) [a_{1, F} V_J(t) + a_{2, F} U_J(t)],$$

$$Z_J = \lambda_{f, \gamma}^J \exp[-(\lambda_0 + \lambda_{f, \gamma}^J + \lambda_{f, \mu}^J)t], \quad (3a)$$

$$V_J = [1 - \exp(-\beta_J t)] / \beta_J, \quad \beta_J \equiv \Lambda_{p\mu d} - (\lambda_{f, \gamma}^J + \lambda_{f, \mu}^J),$$

$$U_J = [1 - \exp(-\alpha_J t)] / \alpha_J,$$

$$\alpha_J \equiv \Lambda_{p\mu d} + \Lambda_d + \Lambda_d' - (\lambda_{f, \gamma}^J + \lambda_{f, \mu}^J).$$

Here $C_{F, J}$ denotes the population of the hyperfine states of the $p\mu d$ molecule;²⁴ the λ_f^J are the partial rates of the fusion reaction; and the $a_{i, F}$ ($i = 1, 2$) are the fitting factors in the population functions of the $d\mu$ -atom hyperfine states,

$$n_F(t) = a_{1, F} \exp[-(\lambda_0 + \Lambda_{p\mu d})t] + a_{2, F} \exp[-(\lambda_0 + \Lambda_{p\mu d} + \Lambda_d + \Lambda_d')t],$$

$$a_{1, 1/2} = \Lambda_d / (\Lambda_d + \Lambda_d'), \quad a_{2, 1/2} = -(2\Lambda_d - \Lambda_d') / 3(\Lambda_d + \Lambda_d'),$$

$$a_{1, 3/2} = \Lambda_d' / (\Lambda_d + \Lambda_d'), \quad a_{2, 3/2} = -a_{2, 1/2}, \quad (3b)$$

where

$$\Lambda_d' = 2\Lambda_d \exp(-560/T) \quad (3c)$$

is the $F = 1/2 \rightarrow F = 3/2$ transition rate.

To estimate the errors resulting from neglect of muon regeneration, we analyzed both the exact solution obtained for a single "effective" reaction rate, and the temporal spectrum of gamma rays obtained by Monte Carlo modeling incorporating the full process kinetics. Both calculations imply that to within 1–2%, neglect of muon regeneration does not affect $\Lambda_{p\mu d}$, but it does reduce the reaction rate $\lambda_{f, \gamma}^{1/2}$ of (1a) by 7–8%. We therefore corrected the final results for the reaction rate accordingly.

In analyzing the gamma-ray temporal distributions using Eqs. (3), we specified the hydrogen temperature and density, took $\lambda_d(T)$ from Refs. 15 and 16, and took the rate $\lambda_{f, \gamma}^{1/2} = 0.056 \mu\text{s}^{-1}$ from Ref. 5. The values of $\lambda_{p\mu d}$ and $\lambda_{f, \gamma}^{1/2}$ were provided by the fits obtained.

Since the data of Refs. 3, 12, and 17 were analyzed under the assumption that $\lambda_{f, \gamma}^{3/2} = 0$, and the value of $\lambda_{p\mu d}$ used in Ref. 17 was obtained through an independent "direct" method,¹³ we first analyzed the case $\lambda_{f, \gamma}^{3/2} = 0$. This was the approximation used to process the data from the first four runs, and it yielded a reaction rate $\lambda_{f, \gamma}^{1/2} = (0.319 \pm 0.013) \mu\text{s}^{-1}$ and a corresponding value $\lambda_{p\mu d} = (5.78 \pm 0.29) \mu\text{s}^{-1}$ (statistical errors), which are close to the results reported in Refs. 3, 12, 13, and 17.

For a full analysis of $\lambda_{f, \gamma}^{3/2}$, we fixed its value at $\lambda_{f, \gamma}^{3/2} = 0.11 \mu\text{s}^{-1}$ (following Refs. 4–6). The partial rate $\lambda_{f, \gamma}^{1/2}$ was varied together with $\lambda_{p\mu d}$ for the data from four runs with a high-density mixture ($\varphi = 1$ and $\varphi = 0.67$). The resulting mean value $\lambda_{f, \gamma}^{1/2} = (0.397 \pm 0.022) \mu\text{s}^{-1}$ was then used to analyze the data from the remaining runs. After correcting for neglect of regeneration, we obtained

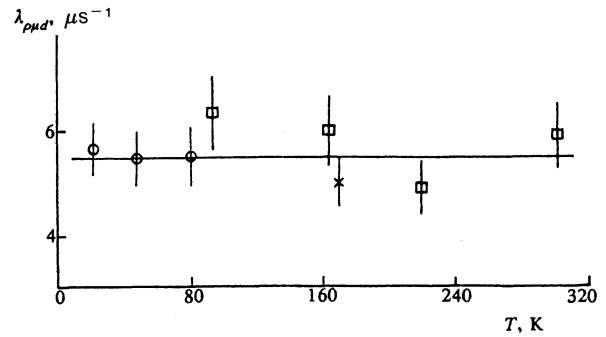


FIG. 5. Measured value of $\lambda_{p\mu d}$ as a function of temperature. Notation as in Fig. 4. The horizontal line corresponds to the mean value (4).

$$\lambda_{f, \gamma}^{1/2} = 0,426 \pm 0,024 \mu\text{s}^{-1},$$

which is somewhat higher than the value reported in Ref. 6, $\lambda_{f, \gamma}^{1/2} = (0.350 \pm 0.020) \mu\text{s}^{-1}$, but is in fairly good agreement with the calculated⁴ value, $\lambda_{f, \gamma}^{1/2} = (0.37 \pm 0.01) \mu\text{s}^{-1}$.

We have plotted the values of $\lambda_{p\mu d}$ derived from our data in Fig. 5. The mean over all runs,

$$\lambda_{p\mu d} = 5,49 \pm 0,19 \pm 0,23 \mu\text{s}^{-1}, \quad (4)$$

is shown by a horizontal line. The first error value in (4) is the statistical uncertainty, and the second is the systematic error induced by imperfect knowledge of the deuterium concentration, the purity of the hydrogen, and several other factors. It is clear from Fig. 5 that our experimental data attest to the temperature independence of $\lambda_{p\mu d}$.

The possible influence of the thermalization of $d\mu$ atoms was assessed on the basis of the fit of the gamma-ray temporal spectra, in which the inverse transition rate Λ_d' was specified for $T = 2000$ K [see Eq. (3c)]. We found that $\lambda_{p\mu d}$ was reduced by approximately 3%.

Combining the statistical and systematic errors in (4), we obtain

$$\lambda_{p\mu d} = 5,49 \pm 0,30 \mu\text{s}^{-1}.$$

This value is in good agreement with previous experimental^{3,6,12,13} and theoretical¹⁹ results.

The authors thank V. B. Belyaev, V. E. Markushin, A. V. Matveenko, and M. P. Faifman for useful discussions.

¹L. Wolfenstein, *Proceedings of the 1960 Conference on High Energy Physics at Rochester*, Interscience, New York (1960).

²S. S. Gershtein, *Zh. Eksp. Teor. Fiz.* **40**, 698 (1961) [*Sov. Phys. JETP* **13**, 488 (1961)].

³E. J. Bleser, E. W. Anderson, and L. M. Lederman, *Phys. Rev.* **132**, 2679 (1963).

⁴J. L. Friar, B. F. Gibbons, and G. L. Payne, *Phys. Rev. Lett.* **66**, 1827 (1991).

⁵L. N. Bogdanova and V. E. Markushin, *Muon Catalyzed Fusion*, Vols. 5, 6 (1990, 1991), p. 189.

⁶S. Petitjean, K. Lou, and P. Ackerbauer, *Muon Catalyzed Fusion*, Vols. 5, 6 (1990, 1991), p. 199.

⁷S. Hara, H. Fukuda, T. Ishihara, and A. V. Matveenko, *Phys. Lett.* **A130**, 22 (1988).

⁸S. Hara, H. Fukuda, and T. Ishihara, *Phys. Rev.* **A40**, 4332 (1989).

⁹V. I. Korobov and S. I. Vinitsky, *Phys. Lett.* **B288**, 21 (1989).

¹⁰V. B. Belyaev and J. Wrzeczianco, *Proc. 12th Intl. Conf. on Few Body Problems in Physics*, Vancouver, B.C., 2–8 July, 1989, North-Holland, Amsterdam (1989), p. 109C.

- ¹¹V. B. Belyaev, O. T. Kartavtsev, and J. Wrzecionco, *Few Body Systems* **7**, 25 (1989).
- ¹²W. Bertl, W. H. Breunlich, and P. Cammel, *Atomkernenergie* **43**, 184 (1983).
- ¹³V. M. Bystritskiĭ, V. P. Dzhelepov, and V. N. Petrukhin, *Zh. Eksp. Teor. Fiz.* **70**, 1167 (1976) [*Sov. Phys. JETP* **43**, 606 (1976)].
- ¹⁴K. A. Aniol, A. J. Noble, and S. Stanislaus, *Muon Catalyzed Fusion*, Vol. 2 (1989), p. 63.
- ¹⁵V. P. Dzhelepov, V. G. Zinov, and S. A. Ivanovskii, *Pis'ma Zh. Eksp. Teor. Fiz.* **53**, 581 (1991) [*JETP Lett.* **53**, 604 (1991)].
- ¹⁶W. H. Breunlich, M. Cargnelli, and P. Cammel, *Muon Catalyzed Fusion*, Vols. 5,6 (1990,1991), p. 149.
- ¹⁷V. M. Bystritskiĭ, V. P. Dzhelepov, and V. N. Petrukhin, *Zh. Eksp. Teor. Fiz.* **71**, 1680 (1976) [*Sov. Phys. JETP* **44**, 881 (1976)].
- ¹⁸A. Adamchak and V. S. Melezhik, *Muon Catalyzed Fusion*, Vol. 4 (1989), p. 303.
- ¹⁹M. P. Faifman, *Muon Catalyzed Fusion*, Vol. 4 (1989), p. 341.
- ²⁰V. M. Bystritskiy, V. P. Dzhelepov, and V. V. Filchenkov, *Proc. Muon Catalyzed Fusion Symposium, Sanibel Island, Florida, 1988*, S. E. Jones, J. Rafelski, H. J. Monkhorst (eds.), *American Institute of Physics Conference Proceedings No. 181*, New York (1989), p. 23.
- ²¹V. M. Bystritskiy, V. P. Dzhelepov, and V. G. Zinov, *Muon Catalyzed Fusion*, Vols. 5,6 (1990,1991), p. 141.
- ²²V. M. Bystritskiĭ, V. B. Granovskii, and V. P. Dzhelepov, *Prib. Tek. Eksp. No. 1*, 50 (1989).
- ²³E. I. Afanasieva, I. V. Balabin, and V. E. Markushin, *Muon Catalyzed Fusion*, Vols. 5,6 (1990,1991), p. 477.
- ²⁴D. D. Bakalov, S. I. Vinitiskiĭ, and V. S. Melezhik, *Zh. Eksp. Teor. Fiz.* **79**, 1629 (1980) [*Sov. Phys. JETP* **52**, 820 (1976)].

Translated by Marc Damashek